Bioorganic & Medicinal Chemistry 21 (2013) 5770–5781

Contents lists available at ScienceDirect

Bioorganic & Medicinal Chemistry

journal homepage: www.elsevier.com/locate/bmc

Spectroscopic, computational modeling and cytotoxicity of a series of *meso*-phenyl and *meso*-thienyl-BODIPYs

Jaime H. Gibbs [a], Larry T. Robins [a], Zehua Zhou [a], Petia Bobadova-Parvanova [b], Michael Cottam [b], Gregory T. McCandless [a], Frank R. Fronczek [a], M. Graça H. Vicente [a,*]

[a] Louisiana State University, Department of Chemistry, Baton Rouge, LA 70803, USA
[b] Rockhurst University, Department of Chemistry, Kansas City, MO 64110, USA

ARTICLE INFO

Article history:
Received 8 May 2013
Revised 2 July 2013
Accepted 9 July 2013
Available online 18 July 2013

Keywords:
BODIPY
PDT
Fluorescence
Phototoxicity
Cellular uptake

ABSTRACT

A series of twenty-two BODIPY compounds were synthesized, containing various *meso*-phenyl and *meso*-thienyl groups, and their spectroscopic and structural properties were investigated using both experimental and computational methods. Further functionalization of the BODIPY framework via iodination at the 2,6-pyrrolic positions was explored in order to determine the effect of these heavy atoms on the photophysical and cytotoxicity of the *meso*-aryl-BODIPYs. BODIPYs bearing *meso*-thienyl substituents showed the largest red-shifted absorptions and emissions and reduced fluorescence quantum yields. The phototoxicity of the BODIPYs in human carcinoma HEp2 cells depends on both the presence of iodines and the nature of the *meso*-aryl groups. Six of the eleven 2,6-diiodo-BODIPYs investigated showed at least a sevenfold enhancement in phototoxicity (IC_{50} = 3.5–28 μM at 1.5 J/cm^2) compared with the non-iodinated BODIPYs, while the others showed no cytotoxicity, while their singlet oxygen quantum yields ranged from 0.02 to 0.76. Among the series investigated, BODIPYs **2a** and **4a** bearing electron-donating *meso*-dimethoxyphenyl substituents showed the highest phototoxicity and dark/phototoxicity ratio, and are therefore the most promising for application in PDT.

1. Introduction

The high versatility of BODIPY (or 4,4-difluoro-4-bora-3a,4a-diaza-*s*-indacene) dyes has led to their investigation as fluorophores in a variety of applications, including biological labelling and imaging, metal ion sensing and as pH indicators.[1–4] Recently BODIPYs have been proposed for application as photosensitizers in the photodynamic therapy (PDT) of cancers.[5,6]

PDT is a process that combines three components, a photosensitizer, light and oxygen, in such a way that energy is transferred from light to molecular oxygen to generate reactive oxygen species, including singlet oxygen, that are highly cytotoxic to tissues.[7,8] Two porphyrin-based macrocycles are FDA-approved as photosensitizers and several other porphyrinoids are under investigation for the PDT treatment of various neoplastic and non-malignant conditions in dermatology, ophthalmology and cardiology.[9,10] Characteristics of 'ideal' photosensitizers include preferential accumulation in target tissue, a triplet state of adequate energy ($E_T \geqslant 95$ kJ mol^{-1}) for efficient energy transfer, high quantum yields of the triplet state (Φ_T >0.4), long triplet state lifetimes (τ_T = 1 μs), high photostability, high absorption coefficients at the therapeutic excitation window (650–800 nm), and low dark but high phototoxicity.[7,8] BODIPY-based dyes can be synthesized with extended π-systems for excitation within the therapeutic window, however their high phototoxicity/low dark toxicity requirement and the structural features that optimize tumor cell uptake and cytotoxicity remain poorly understood.

The incorporation of heavy halogen atoms, such as bromine or iodine, onto the BODIPY platform generates useful precursors for cross-coupling and nucleophilic substitution reactions,[11–13] and can also lead to effective photosensitizers for PDT applications.[5,6] The addition of heavy atoms to the BODIPY core has the potential to cause enhanced intersystem crossing from the singlet to the triplet excited state that controls the production of singlet oxygen, the main cytotoxic species in PDT, due to spin–orbit coupling by the 'heavy atom effect'.[13–15] In particular, the introduction of iodine atoms at the 2- and/or 6-positions of the BODIPY tends to favor intersystem crossing and singlet oxygen generation, while substitution at the 3,5-positions is reported to lead to fluorescence enhancement.[13] Furthermore, the absorption and emission profiles of halogenated BODIPYs are also expected to be red-shifted compared with their non-halogenated analogs.

On the other hand, the use of isotopically and radioactively labeled heavy atoms, such as ^{123}I, ^{124}I, and ^{131}I, can allow iodinated BODIPYs to be utilized in various bioimaging applications. Radioactive isotopically labeled iodine has been effectively used in single photon emission computed tomography (SPECT) and

* Corresponding author. Tel.: +1 225 578 7405; fax: +1 225 578 3458.
E-mail address: vicente@lsu.edu (M.G.H. Vicente).

0968-0896/$ - see front matter © 2013 Elsevier Ltd. All rights reserved.
http://dx.doi.org/10.1016/j.bmc.2013.07.017

positron emission tomography (PET) imaging studies.[16,17] In previous work, ^{123}I nuclei have been successfully used in nuclear medicine including blood flow, myocardial, and thyroid scintigraphy and for uptake measurements in tumors.[18] The use of radioactively labeled iodine has gained popularity in bioimaging for its longer half-life (ca. 13 h) compared with other commonly used radio agents, including fluorine.[19] Incorporation of targeting moieties into the BODIPY platform is usually performed through post-synthetic modifications[20–22] making radioiodine-labeled BODIPYs suitable for potential use in SPECT and PET modalities.

Herein we report the synthesis of a series of eleven photo-stable *meso*-aryl-BODIPYs from 2,4-dimethylpyrrole and various aryl aldehydes. Furthermore, iodination at the 2,6-positions gave the corresponding diiodo-BODIPY derivatives with high yield and selectivity. These 3,5-dimethyl substituted BODIPYs can undergo Knoevenagel condensation reactions with aldehydes to give mono- and di-styryl functionalized long wavelength absorbing BODIPY dyes, within the biological window suitable for PDT.[23–25] In this study we investigated the effects of the *meso*-aryl substituents on the spectroscopic and cytotoxic properties of a series of eleven BODIPYs and their 2,6-diiodo derivatives.

2. Experimental Section

2.1. Chemistry

All reagents and solvents were purchased from either Sigma Aldrich or Alfa Aesar as reagent grade and used without further purification. Reactions were monitored by TLC using 0.2 mm silica with UV indicator (UV254). Column chromatography was performed using Sorbent Technologies 60 Å silica gel (230–400 mesh). All ^{1}H NMR and ^{13}C NMR spectra were obtained using a Bruker DPX-400, AV-400, or DPX-250 spectrometer (400 MHz or 250 MHz for ^{1}H, 100 MHz for ^{13}C) in deuterated chloroform as solvent with trimethylsilane as an internal indicator. Chemical shifts (δ) are reported in ppm with $CDCl_3$ (^{1}H: 7.27 ppm; ^{13}C: 77.16) used as reference. Coupling constants (J) are reported in Hertz (Hz). High resolution ESI and MALDI mass spectra were obtained using an Agilent Technologies 6210 ESI-TOF Mass Spectrometer or a Bruker UltrafleXtreme MALDI-TOF/TOF. Melting points were determined using a MEL-TEMP electrothermal instrument. 5′-Bromo-[2,2′-bithiophen]-5-carbaldehyde was synthesized in 64% yield as previously reported.[26]

2.1.1. General procedure for synthesis of BODIPYs 1–11

In an oven dried flask, 2,4-dimethylpyrrole (0.9990 g, 10.5 mmol) and the corresponding aryl aldehyde (5.0 mmol) were dissolved in dry dichloromethane (DCM, 300 mL). Boron trifluoride diethyl etherate ($BF_3{\cdot}OEt_2$, 0.15 mL) was added drop-wise and the mixture was stirred at room temperature under nitrogen atmosphere for 48 h (until TLC revealed disappearance of the aldehyde). 2,3-Dichloro-5,6-dicyano-*p*-benzoquinone (DDQ, 1.1578 g, 5.1 mmol) in DCM (5 mL) was added to the solution and stirred for 1 h. Triethylamine (3.8216 g, 37.5 mmol) was then added to the mixture and stirred for 30 min followed by the introduction of $BF_3{\cdot}OEt_2$ (6.17 mL, 50 mmol) in DCM (10 mL) and stirred for 3 h. The mixture was poured into water and the organic layer was washed twice with saturated sodium chloride. The organic layer was passed through a bed of anhydrous Na_2SO_4 and the solvent was evaporated under reduced pressure. The resulting residue was passed through a silica plug using dichloromethane as eluent. The solvent was again removed under vacuum and the crude product was purified by silica gel flash chromatography using 30% dichloromethane in petroleum ether.

2.1.1.1. BODIPY 1 (4,4-difluoro-8-phenyl-1,3,5,7-tetramethyl-4-bora-3a,4a-diaza-*s*-indacene). Obtained as a red solid (0.3529 g) in 22% yield, mp: 168–169 °C; ^{1}H NMR (400 MHz, $CDCl_3$) δ 7.49 (dd, J = 5.2 Hz, 1.4, 3H, *o*,*m*-phenyl H), 7.29 (dd, J = 7.2 and 2.2 Hz, 2H, *p*-phenyl H), 5.98 (s, 2H, β-pyrrole H), 2.56 (s, 6H, 3,5-CH_3), 1.38 (s, 6H, 1,7-CH_3); ^{13}C NMR (100 MHz, $CDCl_3$) δ 155.83, 143.56, 142.14, 135.40, 131.84, 129.53, 129.34, 128.35, 121.60, 14.98, 14.73; HRMS (ESI-TOF) m/z 325.1709 $[M+H]^+$, calculated for $C_{19}H_{20}BF_2N_2$: 325.1688. The NMR data is in agreement with that previously reported.[27]

2.1.1.2. BODIPY 2 (4,4-difluoro-8-(3,5-dimethoxyphenyl)-1,3,5,7-tetramethyl-4-bora-3a,4a-diaza-*s*-indacene). Obtained as a red–orange solid (1.1098 g) in 58% yield, mp = 162 °C (decomposes); ^{1}H NMR (400 MHz, $CDCl_3$) δ 6.54 (t, J = 2.0 Hz, 2H, *m*-phenyl H), 6.46 (d, J = 2.0 Hz, 1H, *p*-phenyl H), 5.99 (s, 2H, β-pyrrole H), 3.80 (s, 6H, OCH_3), 2.56 (s, 6H, 3,5-CH_3), 1.55 (s, 6H, 1,7-CH_3); ^{13}C NMR (100 MHz, $CDCl_3$) δ 161.59, 155.46, 143.10, 141.33, 136.57, 131.06, 121.08, 105.90, 100.92, 55.52, 14.54, 14.17; HRMS (ESI-TOF) m/z 385.1894 $[M+H]^+$, calculated for $C_{21}H_{24}BF_2N_2O_2$: 385.1899. The NMR data is in agreement with that previously reported.[28]

2.1.1.3. BODIPY 3 (4,4-difluoro-8-(3, 5-di-tert-butylphenyl)-1,3,5,7-tetramethyl-4-bora-3a,4a-diaza-*s*-indacene). Obtained as a red–orange solid (0.5084 g) in 23% yield, mp = 115 °C (decomposes); ^{1}H NMR (400 MHz, $CDCl_3$) δ 7.47 (t, J = 1.8 Hz, 1H, *p*-phenyl H), 7.13 (d, J = 1.3 Hz, 2H, *o*-phenyl H), 5.98 (s, 2H, β-pyrrole H), 2.56 (s, 6H, 3,5-CH_3), 1.36 (s, 6H, 1,7-CH_3), 1.32 (s, 18H, *t*-butyl H); ^{13}C NMR (100 MHz, $CDCl_3$) δ 155.08, 151.96, 143.25, 143.17, 133.97, 131.52, 122.08, 121.82, 120.99, 35.08, 31.40, 14.56, 14.12; HRMS (ESI-TOF) m/z 437.2977 $[M+H]^+$, calculated for $C_{27}H_{36}BF_2N_2$: 437.2940. The NMR data is in agreement with that previously reported.[29]

2.1.1.4. BODIPY 4 (4,4-difluoro-8-(3,4-dimethoxyphenyl)-1,3,5,7-tetramethyl-4-bora-3a,4a-diaza-*s*-indacene). Obtained a bright red solid (0.4756 g) in 25% yield, mp = 182–183 °C. ^{1}H NMR (400 MHz, $CDCl_3$) δ 6.97 (d, J = 7.8 Hz, 1H, 5-phenyl H), 6.82 (dd, J = 8.7 and 1.5 Hz, 2H, 6-phenyl H), 6.78 (d, J = 1.5 Hz, 2-phenyl H), 5.98 (s, 2H, β-pyrrole H), 3.94 (s, 3H, OCH_3), 3.84 (s, 3H, OCH_3), 2.54 (s, 6H, 3,5-CH_3), 1.47 (s, 6H, 1,7-CH_3); ^{13}C NMR (100 MHz, $CDCl_3$) δ 155.38, 149.79, 149.50, 143.16, 141.58, 131.72, 127.13, 121.11, 120.42, 111.52, 111.07, 56.11, 55.91, 14.57, 14.45; HRMS (ESI-TOF) m/z 385.1893 $[M+H]^+$, calculated for $C_{21}H_{24}BF_2N_2O_2$: 385.1899. The NMR data is in agreement with that previously reported.[30]

2.1.1.5. BODIPY 5 (4,4-difluoro-8-(4-(methoxycarbonyl) phenyl)-1,3,5,7-tetramethyl-4-bora-3a,4a-diaza-*s*-indacene). Obtained a bright red solid (0.4367 g) in 23% yield, mp = 181–182 °C; ^{1}H NMR (400 MHz, $CDCl_3$) δ 8.19 (d, J = 7.9 Hz, 2H, *m*-phenyl H), 7.42 (d, J = 7.9 Hz, 2H, *o*-phenyl H), 5.99 (s, 2H, β-pyrrole H), 3.97 (s, 3H, $COOCH_3$), 2.56 (s, 6H, 3,5-CH_3), 1.35 (1,7-CH_3); ^{13}C NMR (100 MHz, $CDCl_3$) δ 166.47, 156.00, 142.88, 140.21, 139.95, 130.80, 130.37, 128.39, 121.48, 52.40, 14.62, 14.51; HRMS (ESI-TOF) m/z 383.1746 $[M+H]^+$, calculated for $C_{21}H_{22}BF_2N_2O_2$: 383.1742. The NMR data is in agreement with that previously reported.[31]

2.1.1.6. BODIPY 6 (4,4-difluoro-8-(4-bromophenyl)-1,3,5,7-tetramethyl-4-bora-3a,4a-diaza-*s*-indacene). Obtained as a red solid (0.3760 g) in 19% yield, mp = 172–173 °C; ^{1}H NMR (400 MHz, $CDCl_3$) δ 7.65 (d, J = 8.2 Hz, 2H, *m*-phenyl H), 7.18 (d, J = 8.2 Hz, 2H, *o*-phenyl H), 5.99 (s, 2H, β-pyrrole H), 2.55 (s, 6H, 3,5-CH_3), 1.41 (s, 6H, 1,7-CH_3); ^{13}C NMR (100 MHz, $CDCl_3$) δ 155.91, 142.92, 140.03, 133.96, 132.45, 131.19, 129.84 123.27, 121.47, 14.65, 14.61; HRMS (ESI-TOF) m/z 403.0780 $[M+H]^+$, calculated for $C_{19}H_{19}BBrF_2N_2$: 403.0793. The NMR data is in agreement with that previously reported.[32]

2.1.1.7. BODIPY 7 (4,4-difluoro-8-(thiophen-2-yl)-1,3,5,7-tetramethyl-4-bora-3a,4a-diaza-*s*-indacene). Obtained a red solid (0.3298 g) in 20% yield, mp = 190–191 °C; ^{1}H NMR (400 MHz, $CDCl_3$) δ 7.50 (d, J = 5.0 Hz, 1H, 5-thienyl H), 7.14 (t, J = 4.4 Hz, 1H, 4-thienyl H), 6.99 (d, J = 3.2 Hz, 1H, 3-thienyl H), 6.00 (s, 2H, β-pyrrole H), 2.55 (s, 6H, 3,5-CH_3), 1.58 (s, 6H, 1,7-CH_3); ^{13}C NMR (100 MHz, $CDCl_3$) δ 156. 07, 143.50, 134.63, 134.00, 132.40, 127.81, 127.61, 127.41, 121.50, 14.65, 13.55; HRMS (ESI-TOF) m/z 331.1306 $[M+H]^+$, calculated for $C_{17}H_{18}BF_2N_2S$: 331.1252. The NMR data is in agreement with that previously reported.[33]

2.1.1.8. BODIPY 8 (4,4-difluoro-8-([2, 2'-bithiophen]-2-yl)-1,3,5,7-tetramethyl-4-bora-3a,4a-diaza-*s*-indacene). Obtained a dark red solid (0.4180 g) in 20% yield, mp = 157 °C (decomposes); ^{1}H NMR (400 MHz, $CDCl_3$) δ 7.28 (d, J = 3.5 Hz, 1H, 5′-bithienyl H), 7.23 (d, J = 3.5 Hz, 1H, 4-bithienyl H), 7.20 (d, J = 3.5 Hz, 1H, 3-bithienyl H), 7.06 (dd, J = 4.9 and 3.7 Hz, 1H, 3′-bithienyl H), 6.89 (d, J = 3.5 Hz, 1H, 4′-bithienyl), 6.02 (s, 2H, β-pyrrole H), 2.56 (s, 6H, 3,5-CH_3), 1.75 (s, 6H, 1,7-CH_3); ^{13}C NMR (100 MHz, $CDCl_3$) δ 156.28, 143.44, 133.14, 128.65, 127.98, 125.02, 124.33, 123.73, 121.58, 14.66, 13.95; HRMS (ESI-TOF) m/z 413.1116 $[M+H]^+$, calculated for $C_{21}H_{20}BF_2N_2S$: 413.1129.

2.1.1.9. BODIPY 9 (4,4-difluoro-8-(5-bromothiophen-2-yl)-1,3,5,7-tetramethyl-4-bora-3a,4a-diaza-*s*-indacene). Obtained a dark red solid (0.3740 g) in 18% yield, mp = 167–168 °C; ^{1}H NMR (400 MHz, $CDCl_3$) δ 7.10 (d, J = 3.5 Hz, 1H, 4-thienyl-H), 6.77 (d, J = 3.9 Hz, 1H, 3-thienyl-H), 6.01 (s, 2H, β-pyrrole H), 2.54 (s, 6H, 3,5-CH_3), 1.69 (s, 6H, 1,7-CH_3); ^{13}C NMR (100 MHz, $CDCl_3$) δ 156.57, 143.34, 136.32, 132.11, 130.36, 128.43, 121.75, 113.83, 14.65, 13.87; HRMS (ESI-TOF) m/z 409.0315 $[M+H]^+$, Calculated for $C_{17}H_{17}BBrF_2N_2S$: 409.0357.

2.1.1.10. BODIPY 10 (4,4-difluoro-8-(5'-bromo-[2,2'-bithiophen]-2-yl)-1,3,5,7-tetramethyl-4-bora-3a,4a-diaza-*s*-indacene). Obtained as a dark red solid (0.7439 g) from 5′-bromo-[2,2′-bithiophen]-5-carbaldehyde[19] (1.3658 g) in 30% yield, mp = 205 °C (decomposes); ^{1}H NMR (400 MHz, $CDCl_3$) δ 7.14 (d, J = 3.5 Hz, 1H, 4,4′-bithienyl-H), 7.01 (d, J = 3.5 Hz, 1H, 4,4′-bithienyl H), 6.97 (d, J = 3.9 Hz, 1H, 3,3′-bithienyl-H), 6.89 (d, J = 3.9 Hz, 1H, 3,3′-bithienyl-H), 6.03 (s, 2H, β-pyrrole H), 2.56 (s, 6H, 3,5-CH_3), 1.73 (s, 6H, 1,7-CH_3); ^{13}C NMR (100 MHz, $CDCl_3$) δ 156.42, 143.36, 135.64, 133.70, 132.29, 130.75, 128.76, 124.41, 123.96, 121.64, 111.80, 14.67, 13.93; HRMS (ESI-TOF, negative ion) m/z 489.0089 $[M+H]^+$, calculated for $C_{21}H_{17}BBrF_2N_2S_2$: 489.0078.

2.1.1.11. BODIPY 11 (4,4-difluoro-8-pentafluorophenyl-1,3,5,7-tetramethyl-4-bora-3a,4a-diaza-*s*-indacene). Obtained as a red solid (0.3820 g) in 52% yield, mp = 109 °C (decomposes); ^{1}H NMR (400 MHz, $CDCl_3$) δ 6.06 (s, 2H, β-pyrrole H), 2.57 (s, 6H, 3,5-CH_3), 1.62 (s, 6H, 1,7-CH_3); ^{13}C NMR (100 MHz, $CDCl_3$) δ 157.78, 145.26, 142.77, 141.50, 139.44, 137.10, 130.99, 122.73, 122.26, 14.76, 13.57; HRMS (ESI-TOF) m/z 415.1337 $[M+H]^+$, calculated for $C_{19}H_{15}BF_7N_2$: 415.1216. The NMR data is in agreement with that previously reported.[34]

2.1.2. General procedure for Iodination of BODIPYs 1–11

Iodic acid (2 equiv) was dissolved in a minimal amount of water and added drop-wise to a solution of the BODIPY (1 equiv) and iodine (2.5 equiv) in a solution of 50:50 ethanol/DCM (~35 μM solution). The resulting mixture was stirred at 60 °C for 2 h. After cooling, the solvent was evaporated under vacuum and the resulting residue was purified by silica gel column chromatography using 50:50 hexanes/DCM for elution.

2.1.2.1. BODIPY 1a (4,4-difluoro-8-phenyl-2,6-di-iodo-1,3,5,7-tetramethyl-4-bora-3a,4a-diaza-*s*-indacene). Obtained as a red solid (0.1618 g) in 91% yield from 1 (0.100 g, 0.3085 mmol), iodic acid (0.1085 g, 0.6169 mmol), iodine (0.0979 g, 0.7713 mmol), mp = 204–206 °C; ^{1}H NMR (400 MHz, $CDCl_3$) δ 7.54 (dd, J = 5.2 Hz, 1.4, 3H, *o,p*-phenyl H), 7.26 (dd, J = 7.2 and 2.2 Hz, 2H, *m*-phenyl H), 2.65 (s, 6H, 3,5-CH_3), 1.39 (s, 6H, 1,7-CH_3); ^{13}C NMR (100 MHz, $CDCl_3$) δ 156.78, 145.37, 141.38, 134.74, 131.30, 129.54, 129.47, 127.79, 85.65, 16.95, 16.04; HRMS (ESI-TOF) m/z 575.9461 $[M]^+$, calculated for $C_{19}H_{17}BF_2I_2N_2$: 575.9543. The NMR data is in agreement with that previously reported.[35]

2.1.2.2. BODIPY 2a (4,4-difluoro-2,6-di-iodo-8-(3,5-dimethoxyphenyl)-1,3,5,7-tetramethyl-4-bora-3a,4a-diaza-*s*-indacene). Obtained as a red solid (0.0952 g) in 57% yield from **2** (0.100 g, 0.2603 mmol), iodic acid (0.1145 g, 0.6508 mmol), iodine (0.0826 g, 0.6508 mmol), mp = 192–193 °C; ^{1}H NMR (400 MHz, $CDCl_3$) δ 6.59 (t, J = 2.0 Hz, 2H, *m*-phenyl H), 6.41 (d, J = 2.0 Hz, 1H, *p*-phenyl H), 3.81 (s, 6H, OCH_3), 2.65 (s, 6H, 3,5-CH_3), 1.57 (s, 6H, 1,7-CH_3); ^{13}C NMR (100 MHz, $CDCl_3$) δ 161.94, 156.84, 149.46, 145.42, 136.31, 131.12, 105.77, 101.45, 85.58, 55.65, 16.88, 16.06; HRMS (ESI-TOF) m/z 636.9810 $[M+H]^+$, calculated for $C_{21}H_{21}BF_2I_2N_2O_2$: 636.9832.

2.1.2.3. BODIPY 3a (4,4-difluoro-8-(3,5-di-*t*-butylphenyl)-2,6-di-iodo-1,3,5,7-tetramethyl-4-bora-3a,4a-diaza-*s*-indacene). Obtained as a red solid (0.3658 g) in 93% yield from **3** (0.250 g, 0.5729 mmol), iodic acid (0.2016 g, 1.1458 mmol) and iodine (0.1818 g, 1.4323 mmol); ^{1}H NMR (400 MHz, $CDCl_3$) δ 7.54 (t, J = 1.8 Hz, 1H, *p*-phenyl H), 7.08 (d, J = 1.3 Hz, 2H, *o*-phenyl H), 2.66 (s, 6H, 3,5-CH_3), 1.37 (s, 6H, 1,7-CH_3), 1.33 (s, 18H, *t*-butyl H); ^{13}C NMR (100 MHz, $CDCl_3$) δ 156.40, 152.48, 145.35, 142.94, 133.76, 131.39, 122.46, 121.87, 85.45, 35.15, 31.40, 16.69, 15.99; HRMS (ESI-TOF) m/z 688.0730 $[M]^+$, calculated for $C_{27}H_{33}BF_2I_2N_2$: 688.0794.

2.1.2.4. BODIPY 4a (4,4-difluoro-8-(3,4-dimethoxyphenyl)-2,6-di-iodo-1,3,5,7-tetramethyl-4-bora-3a, 4a-diaza-*s*-indacene). Obtained as a red solid (0.3907 g) in 94% yield from **4** (0.250 g, 0.6507 mmol), iodic acid (0.2289 g, 1.3013 mmol), iodine (0.2065 g, 1.6268 mmol), mp = 215–217 °C; ^{1}H NMR (400 MHz, $CDCl_3$) δ 7.02 (d, J = 7.8 Hz, 1H, 5-phenyl H), 6.82 (dd, J = 8.7 Hz, 1.5, 2H, 6-phenyl H), 6.74 (d, J = 1.5 Hz, 2-phenyl H), 3.98 (s, 3H, OCH_3), 3.87 (s, 3H, OCH_3), 2.65 (s, 6H, 3,5-CH_3), 1.49 (s, 6H, 1,7-CH_3); ^{13}C NMR (100 MHz, $CDCl_3$) δ 156.70, 150.10, 149.97, 145.37, 141.28, 131.62, 126.78, 120.33, 111.76, 111.81, 85.58, 56.18, 56.01, 17.07, 16.01; HRMS (ESI-TOF) m/z 635.9840 $[M]^+$, calculated for $C_{21}H_{21}BF_2I_2N_2O_2$: 635.9754. The NMR data is in agreement with that previously reported.[36]

2.1.2.5. BODIPY 5a (4,4-difluoro-2,6-di-iodo-8-(4-(methoxycarbonyl)phenyl)-1,3,5,7-tetramethyl-4-bora-3a,4a-diaza-*s*-indacene). Obtained as a red solid (0.3570 g) in 86% yield from **5** (0.250 g, 0.6541 mmol), iodic acid (0.2301 g, 1.3082 mmol), iodine (0.2075 g, 1.6353 mmol), mp = 215 °C (decomposes); ^{1}H NMR (400 MHz, $CDCl_3$) δ 8.23 (d, J = 7.9 Hz, 2H, *m*-phenyl H), 7.40 (d, J = 7.9 Hz, 2H, *o*-phenyl H), 3.99 (s, 3H, $COOCH_3$), 2.65 (s, 6H, 3,5-CH_3), 1.37 (1,7-CH_3); ^{13}C NMR (100 MHz, $CDCl_3$) δ 166.24, 157.34, 145.07, 139.81, 139.46, 131.34, 130.81, 130.66, 128.24, 86.04, 52.53, 17.14, 16.12; HRMS (ESI-TOF) m/z 634.9663 $[M+H]^+$, calculated for $C_{21}H_{20}BF_2I_2N_2O_2$: 634.9676. The NMR data is in agreement with that previously reported.[37]

2.1.2.6. BODIPY 6a (4,4-difluoro-8-(4-bromophenyl)-2,6-di-iodo-1,3,5,7-tetramethyl-4-bora-3a,4a-diaza-*s*-indacene). Obtained as a red solid (0.4422 g) in 71% yield from 6 (0.250 g, 0.6202 mmol), iodic acid (0.2182 g, 1.2405 mmol), iodine (0.1968 g, 1.5505 mmol), mp = 232 °C (decomposes); ^{1}H NMR

(400 MHz, $CDCl_3$) δ 7.71 (d, J = 8.2 Hz, 2H, *m*-phenyl H), 7.18 (d, J = 8.2 Hz, 2H, *o*-phenyl H), 2.65 (s, 6H, 3,5-CH_3), 1.44 (s, 6H, 1,7-CH_3); ^{13}C NMR (100 MHz, $CDCl_3$) δ 157.27, 145.13, 139.64, 133.69, 132.80, 131.08, 129.66 123.91, 85.99, 17.28, 16.09; HRMS (ESI-TOF) m/z 653.8638 $[M]^+$, calculated for $C_{19}H_{16}BBrF_2I_2N_2$: 653.8648.

2.1.2.7. BODIPY 7a (4,4-difluoro-2,6-di-iodo-8-(thiophen-2-yl)-1,3,5,7-tetramethyl-4-bora-3a,4a-diaza-*s*-indacene).

Obtained as a red solid (0.5997 g) in 79% yield from **7** (0.250 g, 0.7571 mmol), iodic acid (0.2664 g, 1.5142 mmol), iodine (0.2402 g, 1.8928 mmol), mp = 186–187 °C; ^{1}H NMR (400 MHz, $CDCl_3$) δ 7.57 (d, J = 5.0 Hz, 1H, 5-thienyl H), 7.19 (t, J = 4.4 Hz, 1H, 4-thienyl H), 7.00 (d, J = 3.2 Hz, 1H, 3-thienyl H), 2.65 (s, 6H, 3,5-CH_3), 1.59 (s, 6H, 1,7-CH_3); ^{13}C NMR (100 MHz, $CDCl_3$) δ 157.35, 145.65, 134.34, 133.75, 132.25, 128.20, 128.14, 127.97, 86.17, 16.27, 16.11; HRMS (ESI-TOF) m/z 582.9173 $[M+H]^+$, calculated for $C_{17}H_{16}BF_2I_2N_2S$: 582.9185.

2.1.2.8. BODIPY 8a (4,4-difluoro-2,6-di-iodo-8-([2,2'-bithiophen]-2-yl)-1,3,5,7-tetramethyl-4-bora-3a, 4a-diaza-*s*-indacene).

Obtained as a red solid (0.5073 g) in 84% yield from **8** (0.250 g, 0.6063 mmol), iodic acid (0.2133 g, 1.2126 mmol), iodine (0.1924 g, 1.5158 mmol), mp = 195–196 °C; ^{1}H NMR (400 MHz, $CDCl_3$) δ 7.25 (t, J = 3.3 Hz, 1H, 5′-bithienyl H), 7.21 (d, J = 3.9 Hz, 1H, 4-bithienyl H), 7.18 (d, J = 3.4 Hz, 1H, 3-bithienyl H), 6.91 (dd, J = 5.1 and 4.2 Hz, 2H, 3′,4′-bithienyl), 2.66 (s, 6H, 3,5-CH_3), 1.74 (s, 6H, 1,7-CH_3); ^{13}C NMR (100 MHz, $CDCl_3$) δ 157.67, 145.50, 141.83, 139.22, 137.88, 133.23, 129.13, 129.04, 128.09, 125.95, 125.41, 124.67, 86.28, 16.69, 16.14; HRMS (ESI-TOF) m/z 663.8988 $[M+H]^+$, calculated for $C_{21}H_{17}BF_2I_1N_2S_2$: 663.8984.

2.1.2.9. BODIPY 9a (4,4-Difluoro-8-(5-bromothiophen-2-yl)-2,6-di-iodo-1,3,5,7-tetramethyl-4-bora-3a,4a-diaza-*s*-indacene).

Obtained as a red solid (0.0738 g) in 91% yield from 9 (0.050 g, 0.1222 mmol), iodic acid (0.0430 g, 0.2444 mmol), iodine (0.0388 g, 0.3055 mmol), mp = 212 °C (decomposes); ^{1}H NMR (400 MHz, $CDCl_3$) δ 7.15 (d, J = 3.4 Hz, 1H, 4-thienyl-H), 6.79 (d, J = 3.9 Hz, 1H, 3-thienyl-H), 2.65 (s, 6H, 3,5-CH_3), 1.71 (s, 6H, 1,7-CH_3); ^{13}C NMR (100 MHz, $CDCl_3$) δ 158.18, 145.48, 136.18, 132.63, 130.65, 128.79, 114.84, 86.05, 16.63, 16.15; HRMS (ESI-TOF) m/z 660.8246 $[M+H]^+$, calculated for $C_{17}H_{15}BBrF_2I_2N_2S$: 660.8290.

2.1.2.10. BODIPY 10a (4,4-Difluoro-8-(5′-bromo-[2,2′-bithiophen]-2-yl)-2,6-diiodo-1,3,5,7-tetramethyl-4-bora-3a,4a-diaza-*s*-indacene).

Obtained as a red solid (0.2457 g) in 65% yield from **10** (0.250 g, 0.5089 mmol), iodic acid (0.1791 g, 1.0179 mmol), iodine (0.1615 g, 1.2723 mmol), mp = 198 °C (decomposes); ^{1}H NMR (400 MHz, $CDCl_3$) δ 7.17 (d, J = 3.5 Hz, 1H, 4,4′-bithienyl-H), 7.03 (d, J = 3.9 Hz, 1H, 4,4′-bithienyl H), 6.98 (d, J = 3.9 Hz, 1H, 3,3′-bithienyl-H), 6.90 (d, J = 3.5 Hz, 1H, 3,3′-bithienyl-H), 2.65 (s, 6H, 3,5-CH_3), 1.74 (s, 6H, 1,7-CH_3); ^{13}C NMR (100 MHz, $CDCl_3$) δ 157.68, 145.50, 139.38, 137.40, 133.20, 132.42, 132.16, 130.85, 129.13, 124.75, 124.14, 112.25, 86.32, 16.68, 16.15; MS (MALDI-TOF) m/z 741.8490 $[M+H]^+$, calculated for $C_{21}H_{16}BBrF_2I_2N_2S_2$: 741.8089.

2.1.2.11. BODIPY 11a (4,4-Difluoro-8-pentafluorophenyl-2,6-diiodo-1,3,5,7-tetramethyl-4-bora-3a,4a-diaza-*s*-indacene).

Obtained as a red solid (0.0726 g) in 90% yield from 11 (0.050 g, 0.1207 mmol), iodic acid (0.0425 g, 0.2415 mmol), iodine (0.0383 g, 0.3018 mmol), mp = 198 °C (decomposes); ^{1}H NMR (400 MHz, $CDCl_3$) δ 2.68 (s, 6H, 3,5-CH_3), 1.65 (s, 6H, 1,7-CH_3); ^{13}C NMR (100 MHz, $CDCl_3$) δ 159.13, 145.11, 143.74, 142.70, 139.65, 137.07, 130.89, 122.46, 87.05, 16.31, 16.20; HRMS (ESI-TOF) m/z 666.9130 $[M+H]^+$, calculated for $C_{19}H_{13}BF_7I_2N_2$: 666.9150.

2.2. Molecular structures

The crystal structures of BODIPYs **3**, **7**, **1a** and **9a** were determined at low temperature using MoKα radiation on a Nonius KappaCCD (**1a**) diffractometer, CuKα radiation on a Bruker Kappa Apex-II (**3**), or CuKα (**7**) or MoKα (**9a**) radiation on a Bruker Kappa Apex-II DUO diffractometer. For **7**, the thiophene substituent was disordered into two orientations with 0.824(2)/0.176(2) occupancies, and for **9a**, there were two independent molecules in the asymmetric unit. Crystal data: **1a**, $C_{19}H_{17}BF_2I_2N_2$, M = 575.96, monoclinic, a = 11.4673(15), b = 12.9564(15), c = 17.3920(15) Å, β = 130.446(4)°, U = 1966.5(4) Å^3, T = 95 K, space group $P2_1/c$, Z = 4, 16,872 reflections measured, 8604 unique (R_{int} = 0.032) which were used in all calculations. The final R = 0.031 (6345 $I > 2\sigma(I)$ data), $wR(F_2)$ = 0.060 (all data), CCDC 929873; **3**, $C_{27}H_{35}BF_2N_2$, M = 436.38, monoclinic, a = 6.6395(8), b = 12.1074(14), c = 15.139(2) Å, β = 101.284(10)°, U = 1193.5(3) Å^3, T = 90 K, space group $P2/c$, Z = 2, 9239 reflections measured, 2097 unique (R_{int} = 0.042), final R = 0.036 (1887 $I > 2\sigma(I)$ data), $wR(F_2)$ = 0.094 (all data), CCDC 929871; **7**, $C_{17}H_{17}BF_2N_2S$, M = 330.20, monoclinic, a = 6.6059(3), b = 18.5456(9), c = 12.7397(6) Å, β = 92.791(2)°, U = 1558.89(13) Å^3, T = 90 K, space group $P2_1/c$, Z = 4, 14,155 reflections measured, 2797 unique (R_{int} = 0.035), final R = 0.034 (2762 $I > 2\sigma(I)$ data), $wR(F_2)$ = 0.080 (all data), CCDC 929872; **9a**, $C_{17}H_{14}BBrF_2I_2N_2S$, M = 660.88, monoclinic, a = 21.871(2), b = 9.8112(10), c = 19.478(2) Å, β = 107.585(5)°, U = 3984.3(7) Å^3, T = 100 K, space group $P2_1/c$, Z = 8, 162,698 reflections measured, 26,346 unique (R_{int} = 0.052), final R = 0.029 (19,684 $I > 2\sigma(I)$ data), $wR(F_2)$ = 0.060 (all data), CCDC 934829.

2.3. Spectroscopic studies

The photophysical properties of all compounds were determined on solutions prepared by dissolving an adequate amount of crystalline compound in either dichloromethane or tetrahydrofuran. Stock solutions of concentrations between $1.5 \times 10^{-5}$and 5×10^{-5} M were prepared and diluted to appropriate concentrations for collection of absorbance and emission spectra.

Absorption spectra were acquired using a PerkinElmer Lambda 35 UV/vis spectrometer. Measurements obtained for determining optical density, ε, were taken from prepared solutions with concentrations between 7.5×10^{-6} and 2.5×10^{-5} M in order to obtain λ_{max} between 0.5 and 1.0. Fluorescence spectra were recorded by further dilution of stock solutions to between 1.5×10^{-6} and 8×10^{-6} M to achieve an optical density at the excitation wavelength between 0.04 and 0.06 to minimize intermolecular reabsorption and inner-filter effects.[38] Emission measurements were chronicled on a PTI QuantaMaster4/2006SE spectrofluorometer with the slit width set at 2 nm. Rhodamine 6G was used as a standard in calculating the fluorescence quantum yields (φ_F = 0.95 in ethanol). Fluorescence emissions were recorded for all samples, including the standard, after excitation at 480 nm. All measurements, both absorbance and emission, were acquired within 4 h of solution preparation at room temperature (23–25 °C), using a 10 mm path length spectrophotometric cell.

The fluorescent quantum yields (Φ_f) were calculated using the following equation:[39]

$$\Phi_{exp} = \Phi_{ref} \times \frac{F_x[A_{std}]n_x^2}{F_{std}[A_x]n_{std}^2}$$

Φ_{ref} is the fluorescent quantum yield of the standard, F_x is the area under the sample's emission peak, F_{std} is the area under the standard's emission peak, A_{std} is the optical density at which the standard was excited, A_x is the optical density at which the sample was excited, n is the refractive index of the sample's solvent, and n_{std} is the refractive index of the standard's solvent.

2.4. Computational modeling

Electronic structure calculations of BODIPYs **1**–**11** and **1a**–**11a** were carried out using the hybrid Becke's Three Parameter DFT Functional.[40,41] All atoms except iodine were modeled using the 6-31+G(d,p) basis sets. For BODIPY's **1a**–**11a** the iodine atoms were treated using the Stevens–Basch–Krauss (SBK)[42–44] relativistic effective core potentials and the standard CEP-31G basis set. All structures were optimized without symmetry constraints. The Highest Occupied Molecular Orbital (HOMO) and the Lowest Unoccupied Molecular Orbital (LUMO) were rigorously determined without any further approximations. Potential energy surface minima were confirmed with frequency calculations. Rotational energy barriers were determined by performing relaxed scans of the potential energy surface. All calculations were performed using the GAUSSIAN 09 program package.[45]

2.5. Cell studies

The human HEp2 cells used in this study were purchased from ATCC (derived from HeLa, cervical cancer, contamination). The HEp2 cells were maintained in a 50:50 mixture of DMEM:AMEM (Invitrogen) supplemented with 10% FBS (Invitrogen) and 1% antibiotic (penicillin–streptomycin) and 5% CO_2 at 37 °C. A 32 mM BODIPY stock solution was prepared by dissolving the compound in 96% DMSO and 4% Cremophor EL (a nonionic emulsifier). A 2 mL of a 400 μM BODIPY solution containing 1.95% DMSO and 0.05% Cremophor EL was prepared by adding 15 μL DMSO and 25 μL of the 32 mM stock solution into 1960 μL medium. The final solution was sonicated to aid in BODIPY solubilization.

2.5.1. Time-dependent cellular uptake

The HEP2 cells were plated at 15,000 cells per well in a Costar 96-well plate (BD biosciences) and grown overnight. The 10 μM BODIPY solution was prepared by diluting 400 μM stock solution with medium containing 5% FBS and 1% antibiotic. The cells were treated by adding 100 μL/well of the 10 μM BODIPY solution at time periods of 0, 1, 2, 4, 8, and 24 h. The loading medium was removed at the end of the treatments. The cells were washed with 1X PBS, and solubilized by adding 0.25% Triton X-100 in 1X PBS. BODIPY standard curves at 10, 5, 2.5, 1.25, 0.625 and 0.3125 μM concentrations were obtained by diluting 20 mM BODIPY solution with 0.25% Triton X-100 in 1× PBS. A cell standard curve was prepared using 10,000, 20,000, 40,000, 60,000, 80,000, and 100,000 cells per well. The cells were quantified using theCyQuant Cell Proliferation Assay (Life Technologies). The compound and cell number were determined using a FluoStar Optima micro-plate reader (BMG LRBTEH), with wavelengths 355/520 and 485/520 nm. Cellular uptake was expressed in terms of nM compound per cell.

2.5.2. Dark cytotoxicity

The HEp2 cells were placed in a 96-well plate as above, with BODIPY concentrations of 400, 200, 100, 50, 25, 12.5, and 0 μM, five repetitions for each concentration, and then incubated at 37 °C. After 24 h incubation, the compound was removed by washing the cells with 1X PBS and replaced with media containing 20% Cell Titer Blue. The cells were incubated for an additional 4 h at 37 °C. The viable cells were measured using fluorescence at 570/615 nm using a FluoStar Optima micro-plate reader. The dark toxicity was expressed in terms of the percentage of viable cells.

2.5.3. Phototoxicity

The concentration range of 200, 100, 50, 25, 12.5, 6.25, 3.125 and 0 μM was used for the phototoxicity experiments. The HEp2 cells were placed in 96-well plates as described above, and treated with compound for 24 h at 37 °C. After the 24 h treatment, the loading media was removed. The cells were washed with media, and then refilled with fresh media. The cells were placed on ice and exposed to 610 nm LP filter light from a 100 W halogen lamp filtered through a 610 nm long pass filter (Chroma) for 20 min. An inverted plate lid filled with cold water to a depth of 5 mm acted as an IR filter. The total light dose was approximately 1.5 J/cm^2. After exposure to light, the cells were returned back to the incubator for 24 h. After 24 h incubation, the medium was removed and replaced with medium containing 20% of Cell Titer Blue. The cells were incubated for an additional 4 h. The viable cells were measured by fluorescence at 570/615 nm using a FluoStar Optima micro-plate reader. The phototoxicity was expressed in terms of the percentage of viable cells.

2.5.4. Comparative singlet oxygen quantum yields

To each well of a 6-well plate was added 2 mL containing 50 μM of 1,3-diphenylisobenzofuran (DPBF) and 5 μM of each photosensitizer in DMSO. The plate was irradiated using a 71 W filtered light source of >500 nm with a Schott glass 500 nm long-pass yellow filter for 1 h. At 15 min increments, 200 μL aliquots were removed from each of the six wells and the absorbance was measured at 410 nm. The rate of singlet oxygen generation was determined by the decrease in absorbance of DPBF over time. Control solutions of DPBF–DMSO (negative control) and DPBF–methylene blue–DMSO (reference standard) were irradiated under the previous mentioned conditions. Singlet oxygen quantum yields were determined using the following equation:

$$\Phi_{\Delta(x)} = \Phi_{\Delta(\mathrm{std})} \times \frac{S_x}{S_{\mathrm{std}}}$$

$\Phi_{\Delta(U)}$ is the singlet oxygen quantum yield of the sample, $\Phi_{\Delta(\mathrm{std})}$ is the singlet oxygen quantum yield of the standard (methylene blue, 0.52), S_U is the slope of the plot of absorbance versus time of the sample, and s_{std} is the slope of the plot of absorbance versus time of the standard.[15]

3. Results and discussion

3.1. Synthesis and structural characterization

Eleven *meso*-aryl BODIPYs (**1**–**11**) were synthesized from commercially available 2,4-dimethylpyrrole and the corresponding aryl aldehyde, following a three-step one-pot procedure often used for BODIPY synthesis[46] (Scheme 1). First, two pyrrole units were condensed with the aryl aldehyde in dichloromethane in the presence of $BF_3{\cdot}OEt_2$, then the resulting dipyrromethanes were oxidized using DDQ and finally the dipyrromethenes were complexed with excess $BF_3{\cdot}OEt_2$ under basic conditions. Following work-up, the BODIPYs were purified by silica gel column chromatography and re-crystallized, to give the target compounds in 18 to 58% yields. All starting aldehydes are commercially available except 5′-bromo-[2,2′-bithiophen]-5-carbaldehyde that was used in the synthesis of BODIPY **10**, which was prepared from [2,2′-bithiophen]-5-carbaldehyde in 64% yield, using a published procedure.[25] Subsequent iodination of BODIPYs **1**–**11** to produce **1a**–**11a** was accomplished through electrophilic substitution at the 2,6-positions using iodic acid in ethanol and dichloromethane at 60 °C for 2 h, in 57–94% yield.[13,15] These *meso*-aryl BODIPYs were synthesized to investigate the effects of halogenation and the nature of the *meso*-aryl groups on the photophysical and cytotoxic properties of the BODIPYs. *Meso*-Substitution has been observed to increase the photostability of the BODIPY[47,48] and iodination at the 2,6-positions is reported to enhance intersystem crossing by the 'heavy atom effect,' and consequently the phototoxicity of the BODIPYs.[13–15] On the other hand, halogenation at the 3,5-positions or at the BODIPY *meso*-phenyl or *meso*-thienyl substituents is not expected to significantly affect the cytotoxicity of the compounds.

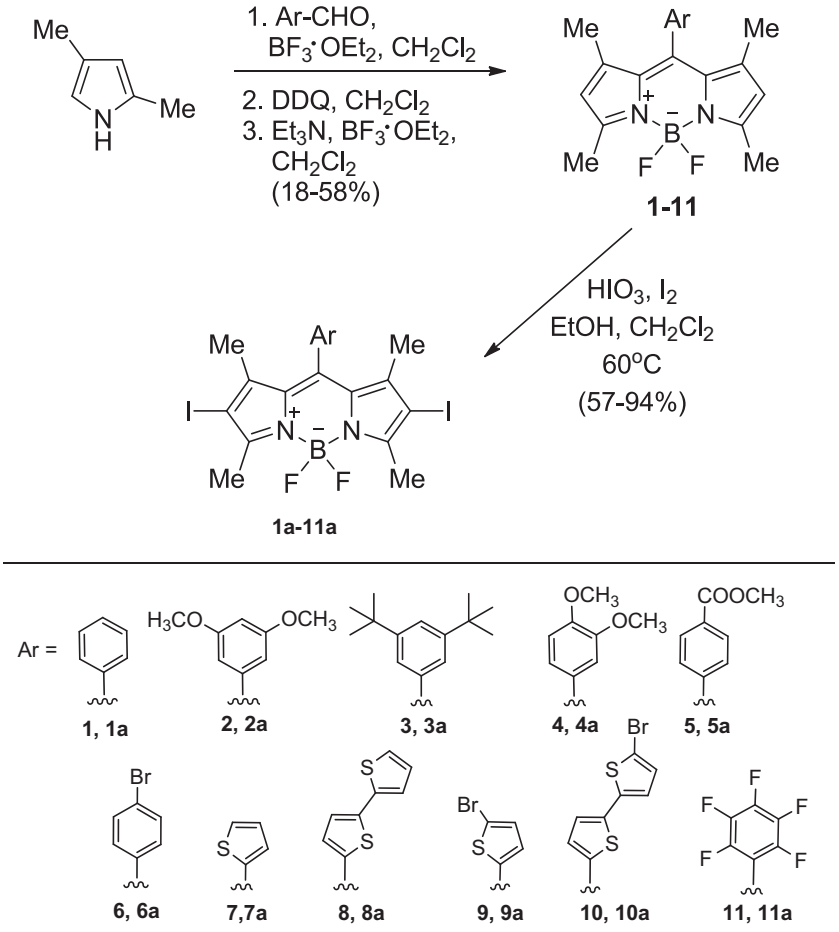

Scheme 1.

All BODIPYs were characterized by ^{1}H and ^{13}C NMR, HRMS and, in the case of **3**, **7**, **1a**, and **9a**, by X-ray crystallography (Fig. 1). Analysis of the NMR spectra (see Supplementary data, Figs. S11–S31) shows the twofold symmetry of the BODIPY core. Single peaks for the 2,6-hydrogens, the 1,7- and 3,5-dimethyl groups on the ^{1}H NMR spectra and the appearance of signals for only half of the BODIPY core's carbons in ^{13}C NMR, indicate a plane of symmetry extending through the boron and carbon-8 (*meso*-position). The upfield shift of the 1,7-dimethyl groups (at approximately 1.6 ppm) compared with the 3,5-dimethyls (at approximately 2.5 ppm) is in part due to the shielding by the *meso*-aryl groups. The disappearance of the 2,6-hydrogens (at ~6.0 ppm) in the ^{1}H NMR spectra indicated complete iodination; additional evidence was provided by the shift of the carbon atoms bearing these hydrogens in ^{13}C NMR, from 120 to 85 ppm.

Single crystals of two β-free and two di-iodo BODIPYs suitable for X-ray analyses were grown from dichloromethane, acetone, or chloroform-*d* and their molecular structures are shown in Figure 1. X-ray analyses reveal the expected approximate twofold symmetry of all four compounds, with two conformers of BODIPYs **7** and **9a** being elucidated (only one of each is shown in Fig. 1). This suggests that the thienyl group located at the *meso*-position has greater rotational freedom compared with the *meso*-phenyl substituent. The BODIPY core and *meso*-substituent lie nearly perpendicular to one another in the molecule's most relaxed form, which reduces the steric strain caused by the 1,7-dimethyl groups.[49] The boron possess nearly tetrahedral geometry with the two fluorines lying perpendicular to the BODIPY core.

In comparison to previously reported boron-dipyrromethene compounds, the BODIPY cores of **1a**, **3**, **7** and **9a** adopt expected bond lengths, planarity, and orthogonal dihedral angles of the F atoms relative to the C_9N_2B (excluding peripheral H atoms and substituents) aromatic framework. The dihedral angles of the *meso*-substituents are also nearly 90° out-of-plane of the BODIPY core in the four crystal structures (**1a** 88.01(5)°; **3** 78.60(4)°; **7** two partially occupied orientations: 82.8(2)° and 84.19(11)°; **9a** two independent molecules 82.83(3)° and 89.54(2)°). Intermolecular halogen-halogen bonding exist in the iodinated BODIPYs **1a** (F···I 3.108(2) Å) and in **9a** (F···Br 2.903(1) and 2.971(1) Å; I···Br 3.598(1) and 3.717(1) Å). Intramolecular hydrogen bonding (C–H 0.98 Å, H···F 2.51 Å, C···F 3.1982(16) Å, C–H···F 127°) between the F atoms with a H atom of a methyl group (on the BODIPY core's α-carbon site) is present in BODIPY **3**.

For BODIPY **7**, the average structure contains two partially occupied orientations. The orientations can be modeled using static (positional) disorder with a refined occupancy ratio of 0.824(2):0.176(2) for two of the thiophene atoms (S and one of the C atoms). In Figure 1, only one of the two orientations is shown. The crystal structure of BODIPY **3** has been previously reported in literature and Cambridge Structural Database (CCDC 712038) based on room temperature measurements.[29] Other close matches can be found for two other crystal structures (**1a** and **7**) determined in this study. These close matches (CCDC 812643 and 856179) have been characterized by others and are extensions of **1a** (with a *meso*-mesityl group, instead of a phenyl) and **7** (with additional quinolin-2-yl on the thiophene's other α-carbon atom).[50,51]

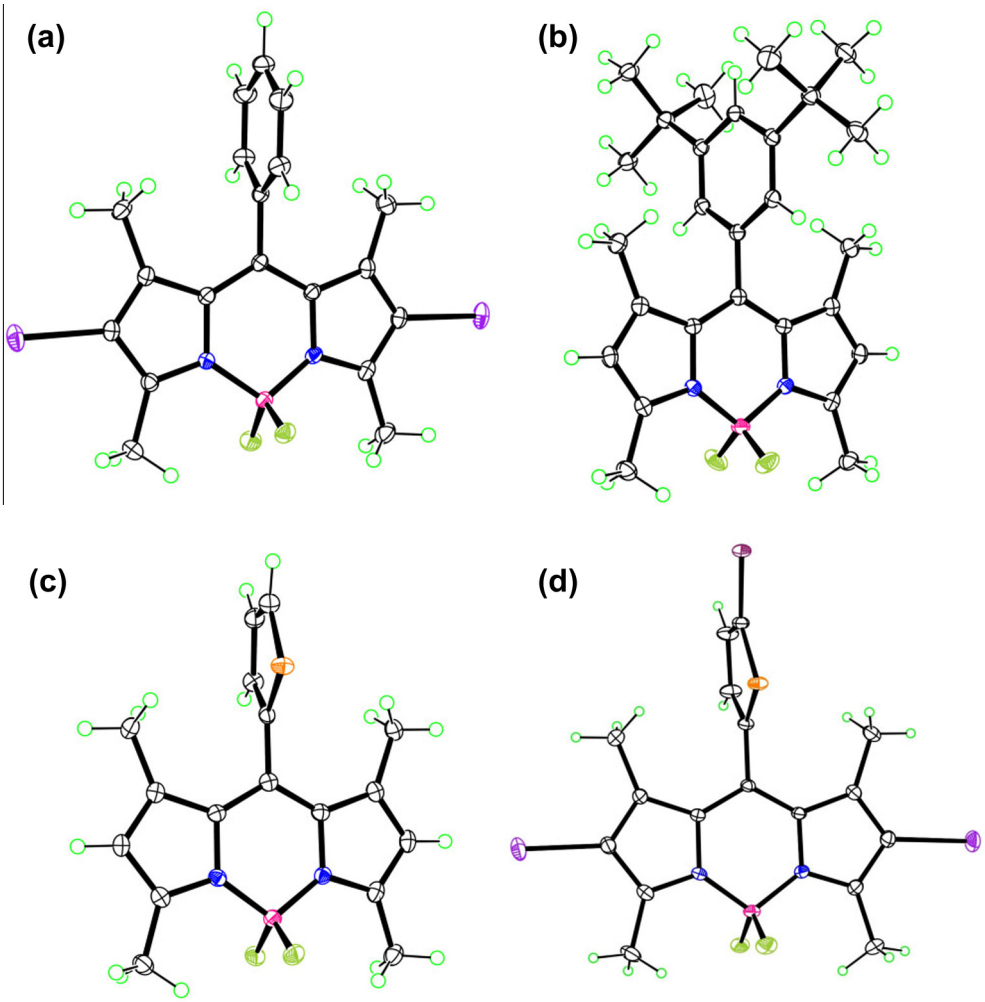

Figure 1. Molecular structures of BODIPYs **1a** (a), **3** (b), **7** (c), and **9a** (d) from X-ray crystal structure determinations. Ellipsoids are drawn at the 50% probability level.

The symmetric nature of the BODIPYs shown by NMR and X-ray crystallography were confirmed by computational modeling. Although no symmetry constraints were used in the calculations and the starting geometries were not symmetric, the optimized geometries of BODIPYs are nearly symmetric (e.g., C_2 for BODIPY **3** and C_s for BODIPY **7**). The BODIPY core and *meso*-substituent form angles between 89.9° and 90.1°.

3.2. Spectroscopic properties and computational studies

The spectroscopic properties of BODIPYs **1**–**11** and **1a**–**11a** were evaluated in dichloromethane and THF, and the results obtained are summarized in Table 1 and also shown in Supplementary data, Figures S1–S6. Little to no solvent effect was observed for these two solvents in the absorption and emission maxima wavelengths. Such lack of influence by the polarity of the solvent indicates that the permanent dipole moments of the BODIPYs do not change between the ground state and the excited state.[52] The synthesized β-free, *meso*-aryl BODIPYs display absorptions between 499 < λ_{abs} < 517 nm and emission bands between 507 < λ_{em} < 530 nm. BODIPYs **1**–**11** show typical fluorescence in the green/yellow spectral region with fluorescence quantum yields in the range 0.03–1.0. The *meso*-thienyl- and pentafluorophenyl BODIPYs exhibited the largest red-shifted profiles and the lowest quantum yields of this series of compounds due to the presence of the sulfur and five fluorines, respectively, which impact the conjugation of the BODIPY π-system (see below).

Incorporation of iodines onto the BODIPY core, as in compounds **1a**–**11a**, causes a shift in the absorption and emission profiles to longer wavelengths, into the orange/red spectral region, and decrease the fluorescence quantum yields, as previously observed.[13–15] The trend observed in the β-free BODIPYs is also seen in their di-iodo analogs with absorption and emisson profiles becoming more red-shifted with the incorporation of thienyl- and pentafluorophenyl-groups. All compounds displayed high extinction coefficients, in the order of 23,000–118,000 M^{-1} cm^{-1} (log ε values between 4.34 and 5.07), and Stokes' shifts in the range 5–20 nm. BODIPYs **7**–**11** and **7a**–**11a**, bearing *meso*-thienyl and pentafluorophenyl substituents, displayed greater red-shifted absorptions and emissions (by 13–41 nm) compared with the other *meso*-phenyl BODIPYs **1**–**6** and **1a**–**6a**. The electron-withdrawing effects of the S and the five F atoms on the *meso*-substituent of BODIPYs **7**–**11** and **7a**–**11a** tend to stabilize the LUMO via delocalization of the electron density (see below).[53] This causes a decrease in the energy of the LUMO, decreasing the HOMO–LUMO gap, and therefore increasing the absorbance and emission maxima wavelengths.

This effect was examined computationally (details of the theoretical level are given the Section 2). The calculated HOMO–LUMO gaps are listed in Table 2, along with the HOMO and LUMO energies. Indeed, for BODIPYs **5**–**11** the LUMO decreases gradually. However, this is not the sole effect determining the gap. In addition to LUMO lowering, the HOMO varies substantially. Therefore, the combination of the HOMO and LUMO effects determine the observed trend.

Table 1
Spectral properties of *meso*-aryl BODIPYs **1**–**11** and 2,6-diiodo-BODIPYs **1a**–**11a** in dichloromethane and THF (in parenthesis), at room temperature

BODIPY	A λ_{max}/nm	log ε (M.L)	Emission λ_{max}/nm	Φ_f	Stokes' shift (nm)
1	501	4.98	511	0.63	10
	(501)	(4.84)	(509)	(0.79)	(8)
2	502	4.78	510	1.00	8
	(501)	(4.86)	(510)	(0.99)	(9)
3	499	4.66	507	0.97	8
	(499)	(4.60)	(507)	(0.73)	(8)
4	501	4.90	510	0.94	9
	(501)	(4.92)	(509)	(0.93)	(8)
5	503	4.80	513	0.56	10
	(502)	(4.81)	(512)	(0.43)	(10)
6	503	4.84	513	0.84	10
	(502)	(4.90)	(511)	(0.53)	(9)
7	513	4.73	520	0.11	7
	(513)	(4.84)	(520)	(0.09)	(7)
8	515	4.34	523	0.03	8
	(515)	(4.57)	(520)	(0.04)	(5)
9	516	5.07	524	0.12	8
	(516)	(4.89)	(524)	(0.10)	(8)
10	516	4.66	522	0.06	6
	(515)	(4.76)	(524)	(0.06)	(9)
11	517	4.57	530	0.91	13
	(516)	(4.77)	(528)	(1.00)	(12)
1a	534	4.97	550	0.05	16
	(533)	(4.92)	(546)	(0.04)	(13)
2a	535	4.89	549	0.07	14
	(534)	(4.94)	(547)	(0.05)	(13)
3a	531	4.84	546	0.06	15
	(531)	(4.83)	(546)	(0.04)	(15)
4a	534	4.96	546	0.05	12
	(532)	(4.88)	(546)	(0.04)	(14)
5a	537	4.82	554	0.05	17
	(536)	(4.77)	(555)	(0.04)	(19)
6a	537	4.81	554	0.04	17
	(536)	(4.84)	(553)	(0.03)	(17)
7a	548	4.37	561	0.04	13
	(548)	(4.68)	(561)	(0.03)	(13)
8a	551	4.59	565	0.01	14
	(550)	(4.60)	(566)	(0.01)	(16)
9a	553	5.07	570	0.03	17
	(553)	(5.05)	(571)	(0.02)	(18)
10a	552	4.87	569	0.01	17
	(551)	4.81)	(571)	(0.01)	(20)
11a	558	4.80	576	0.04	18
	(557)	(4.76)	(571)	(0.03)	(19)

In general, the computational models predict that the eleven BODIPYs will be grouped into three groups: BODIPYs **1**–**6** with gaps around 3.0 eV, BODIPYs **7**–**11** with gaps around 2.9 eV, and BODIPY **10a** with significantly lower gap of 2.7 eV (see Fig. 2). Similar tendencies are seen for the di-iodo BODIPYs; BODIPYs **1a**–**6a** with gaps around 2.9 eV, BODIPYs **7a**–**11a** with gaps around 2.8 eV, and BODIPY **10a** having again significantly lower gap of 2.7 eV. This theoretical prediction is in excellent agreement with the experimentally measured red-shifts of the *meso*-thienyl-BODIPYs **7**–**10** and the *meso*-pentafluorophenyl-BODIPY **11**, and the most pronounced red-shift of the di-iodo-BODIPY **10a**. In general, the di-iodo substitution lowers both the HOMO and LUMO, with the effect on LUMO being slightly more emphasized. The overall effect is to lower slightly the HOMO–LUMO gap, which is in excellent agreement with the experimentally observed red-shifts for all di-iodo BODIPYs when compared with their β-free analogs.

It was also observed that the fluorescence quantum yields for the *meso*-phenyl BODIPYs **1**–**6** and **11** ($0.4 < \varphi_F < 1.0$) were greater than for the *meso*-thienyl BODIPYs **7**–**10** ($0.04 < \varphi_F < 0.12$). Due to the smaller size of the *meso*-group, the thienyl substituent has greater freedom of rotation, which increases the amount of energy lost to non-radiative decay. This spinning motion increases the energy of the system which, in turn, decreases the number of photons that become excited and relax via fluorescence. Negligible effects were caused by the change of solvent. Nevertheless, these results suggest that the *meso*-phenyl BODIPYs with appropriate functionalization may serve as significantly brighter fluorophores in aqueous media than the *meso*-thienyl derivatives. Furthermore, incorporating a longer chain group in the *meso*-position increases the degree of rotational freedom, which also decreases the fluorescence quantum yield as indicated by the results obtained for BODIPYs **7** ($\varphi_F = 0.09–0.11$) and **8** ($\varphi_F = 0.03–0.04$).

Addition of bromine onto the *meso*-thienyl group has only a slight effect on the fluorescence quantum yield, as observed for BODIPYs **7** ($\varphi_F = 0.11$) and **9** ($\varphi_F = 0.12$) in dichloromethane. This result suggests that addition of heavy atoms, such as bromine, onto the *meso*-substituent has little effect on the fluorescence quantum yield, while incorporation of iodines at the 2,6-positions of the BODIPY core, and of *meso*-thienyl groups, significantly decrease the fluorescence quantum yields. With the exception of the fluorines on the *meso*-pentafluorophenyl-BODIPY **11**, the quantum yields significantly decline (**1a**–**11a**, $0.01 < \varphi_F < 0.07$).

The rotational freedom of different *meso*-substituents in vacuum and in dichloromethane was studied computationally at the B3LYP/6-31+G (d,p) level for BODIPYs **1**–**11**. The energy barriers for the rotation of the *meso*-aryl group are given in the last column of Table 2. For most compounds, there is a clear correlation between the rotational barrier and the fluorescence quantum yield (Fig. 3). The *meso*-thienyl group in BODIPYs **7**–**10** can easily rotate with a barrier of only 14–16 kcal/mol, which explains the low

Table 2
Theoretically calculated energies of HOMO (a.u.), LUMO (a.u.), HOMO–LUMO gap, E_g (eV), and *meso*-group rotational barrier, ΔE_{rot} (kcal/mol) in vacuum and in dichloromethane (in parentheses), for BODIPYs **1**–**11a**

BODIPY	HOMO	LUMO	E_g	ΔE_{rot}
1	−0.2072	−0.0976	2.98	20.3 (19.7)
2	−0.2028	−0.0931	2.98	21.0 (20.6)
3	−0.2048	−0.0948	2.99	21.7 (21.2)
4	−0.2068	−0.0973	2.98	24.2 (18.6)
5	−0.2107	−0.1013	2.98	20.5 (20.2)
6	−0.2112	−0.1020	2.97	25.3 (25.0)
7	−0.2090	−0.1030	2.88	15.3 (14.4)
8	−0.2093	−0.1035	2.88	13.6 (12.5)
9	−0.2124	−0.1073	2.86	15.8 (15.2)
10	−0.2113	−0.1058	2.87	14.1 (13.3)
11	−0.2189	−0.1134	2.87	33.0 (33.0)
1a	−0.2159	−0.1106	2.87	—
2a	−0.2117	−0.1061	2.87	—
3a	−0.2136	−0.1076	2.88	—
4a	−0.2152	−0.1094	2.88	—
5a	−0.2188	−0.1139	2.85	—
6a	−0.2195	−0.1147	2.85	—
7a	−0.2175	−0.1157	2.77	—
8a	−0.2173	−0.1155	2.77	—
9a	−0.2204	−0.1190	2.76	—
10a	−0.2222	−0.1222	2.72	—
11a	−0.2260	−0.1253	2.74	—

quantum yield observed for this series of compounds. Heavy atom substitution does not have significant effect on the rotational barrier, which is in agreement with the negligible changes observed in the quantum yield. Taking the solvent into account slightly lowers the rotational barriers but the effect is small and the tendency remains very similar.

BODIPYs **1** and **5** exhibit intermediate rotational barriers and intermediate fluorescence quantum yields. Having a *meso*-phenyl group with substituents at the *meta*-position (OCH_3 or *t*Bu) hinders the rotation and results in significantly higher quantum yields, compared with substituents at the *para*-position. BODIPYs **2**, **3**, **4**, and **6** experience rotational barriers of 20–24 kcal/mol, which is comparable to the kinetic energy at room temperature. The F_5-substituted BODIPY **11** deviates from the relationship to the highest extent probably due to the strong electron-withdrawing character of the *meso*-pentafluorophenyl group. Still, it shows the highest rotational barrier and a large fluorescence quantum yield.

3.3. Cellular properties

The cytotoxicity of a select group of β-free BODIPYs (**5**, **7**, **8** and **10**) and of all 2,6-di-iodo-BODIPYs were investigated in human HEp2 cells using the Cell Titer Blue assay, and the results obtained are summarized in Table 3 (see also Figs. S7–S10 of the Supplementary data). All but one BODIPY (**10a**, IC_{50} = 8 μM) were found to be non-toxic in the dark, with determined IC_{50} values, from dose–response curves, above 400 μM. Upon exposure to a low light dose (1.5 J/cm^2) all the β-free BODIPYs investigated showed low cytotoxicity (IC_{50} >80 μM) in agreement with previous investigations.[15,48] Among the 2,6-diiodo-BODIPYs, **1a**, **2a**, **4a**, **6a**, **7a** and **10a** showed IC_{50} values between 3.5 and 28 μM, while all others (**3a**, **5a**, **8a**, **9a** and **11a**) showed IC_{50} >200 μM. This is a surprising result, since the 2,6-diiodo-BODIPYs previously investigated are

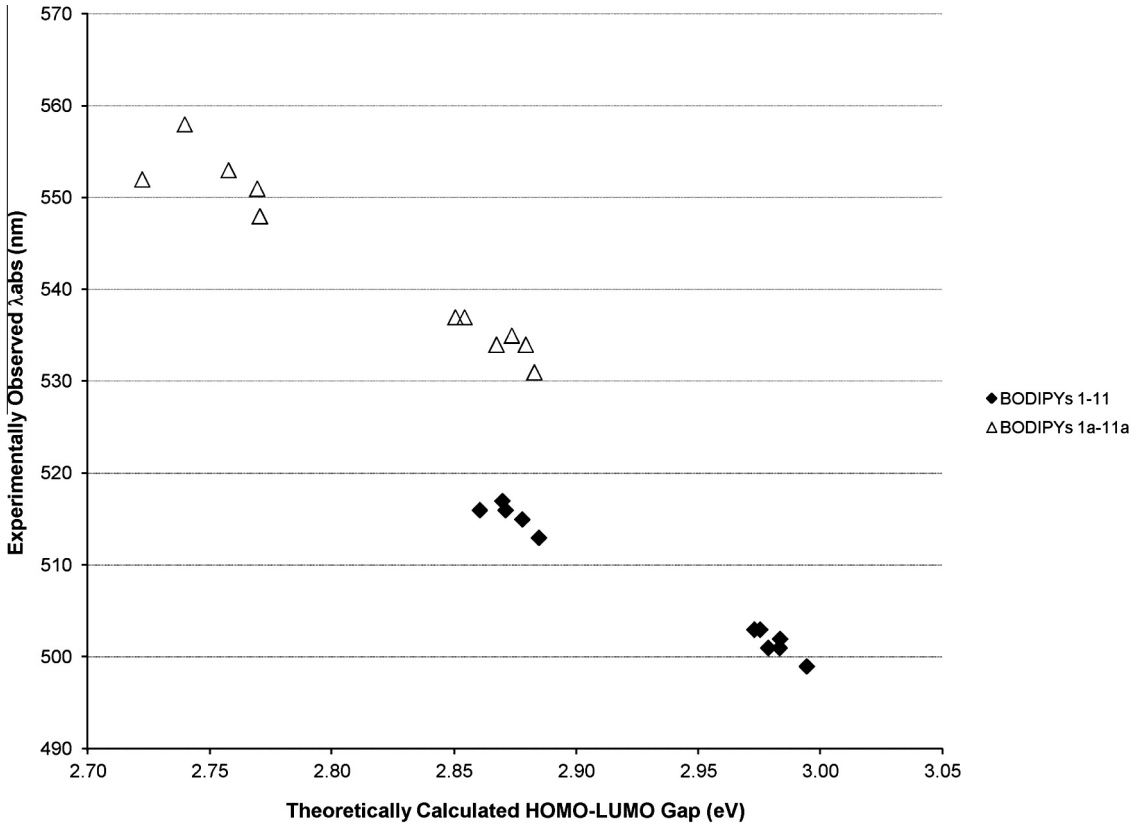

Figure 2. Experimentally observed absorption wavelengths versus the theoretically calculated HOMO–LUMO gap.

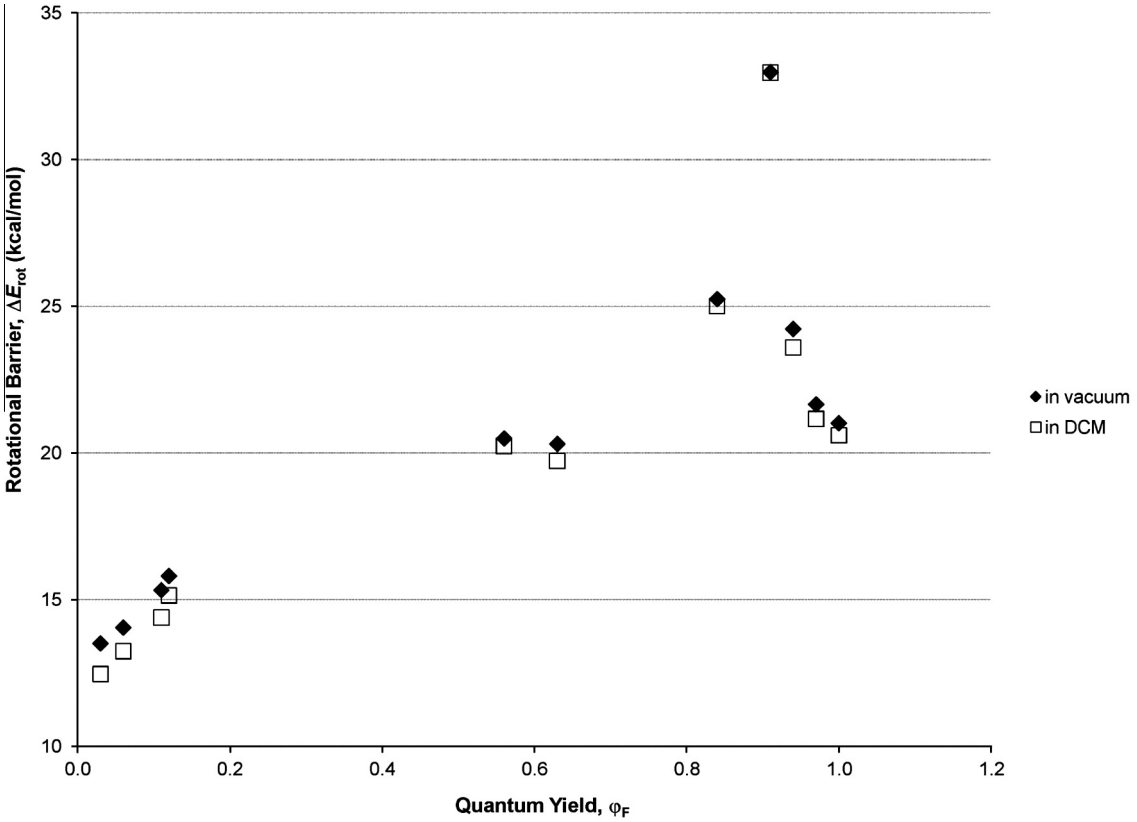

Figure 3. Theoretically calculated *meso*-aryl group rotational barrier (in vacuum and in dichloromethane) versus the experimentally observed quantum yield.

reported to have high phototoxicity,[14,15] attributed to the 'heavy atom effect,' and cleary shows the effect of the *meso*-aryl groups. In particular, BODIPYs **2a**, **4a** and **10a** bearing *meso*-dimethoxyphenyl or bromo-bithienyl substituents show the highest phototoxicity (IC_{50} = 3.5–7.5 μM at 1.5 J/cm^2) and moderate relative rates of singlet oxygen generation (see below); among these, BODIPYs **2a** and **4a** are the most promising for PDT applications due to their high dark/phototoxicity ratio (>50). The observed high phototoxicity of BODIPY **10a** is likely attributed to its substantial dark toxicity. On the other hand, BODIPYs **3a**, **5a**, **8a**, **9a** and **11a** showed no dark/photo cytotoxicities and could therefore find application as radioiodine-labeled imaging agents for SPECT and PET, provided they are deemed to possess specific cellular targeting attributes not yet investigated.

The high dark and phototoxicity observed for BODIPY **10a** might be in part due to its remarkably higher cellular uptake, as shown in Figure 4. On the other hand, BODIPYs **2a** and **4a** were the least accumulated within HEp2 cells, although they were also highly phototoxic, which might be due to their binding to certain protein lipophilic sites.[54] Preliminary results (not shown) reveal that all the phototoxic BODIPYs (**1a**, **2a**, **4a**, **6a**, **7a** and **10a**) localized subcellularly partly within mitochondria, the cell 'power house'.[55] In particular, the role played by mitochondria in apoptosis, the process of programmed cell death, makes these cellular organelles highly desirable targets for PDT.[56] These results are in agreement with a previous study[15] that shows preferential localization of a *meso*-propionate-2,6-diiodo-BODIPY in the mitochondria of HSC-2 cells.

3.4. Singlet oxygen generation studies

The singlet oxygen quantum yields were determined in DMSO for compounds **5**, **7**, **8**, **10**, and **1a**–**11a** by measuring the change in absorbance of singlet oxygen acceptor 1,3-diphenylisobenzofuran (DPBF) in the presence of photosensitizer produced singlet oxygen.[15,57] The change in the 410 nm absorbance of DPBF (at an initial concentration of 50 μM) was measured in 15 min intervals over the course of 1 h, and each photosensitizer was referenced to an equivalent concentration of methylene blue. The singlet oxygen quantum yields ranged from 0.02 (for **7a**) to 0.76 (for **1a**), in agreement with literature,[58] as shown in Table 3. The most phototoxic BODIPYs **2a**, **4a** and **10a** were found to be moderate singlet oxygen generators (Φ_Δ = 0.40, 0.38 and 0.34, respectively) while all other 2,6-diiodo-BODIPYs had Φ_Δ <0.32, with exception of **1a**. Although BODIPY **1a** has the highest singlet oxygen generation rate of this series of compounds, it was not among the four most

Table 3
Comparative singlet oxygen quantum yields (relative to methylene blue), dark and phototoxicity (at 1.5 J/cm^2 light dose) of selected BODIPYs toward HEp2 cells using the Cell Titer Blue assay

BODIPY	Dark toxicity IC_{50} (μM)	Phototoxicity IC_{50} (μM)	Ratio	Φ_Δ
5	>400	>100	>4	0.18
7	>300	>100	>3	0.10
8	>400	>100	>4	0.29
10	>300	82	>3.5	0.38
1a	>400	27	>15	0.76
2a	>400	4.0	>100	0.40
3a	>400	>200	>2	0.32
4a	>400	7.5	>53	0.38
5a	>400	>200	>2	0.27
6a	>400	28	>15	0.31
7a	>400	14	>30	0.02
8a	>400	>200	>2	0.27
9a	>400	>200	>2	0.10
10a	8	3.5	2.3	0.34
11a	>400	>200	>2	0.19

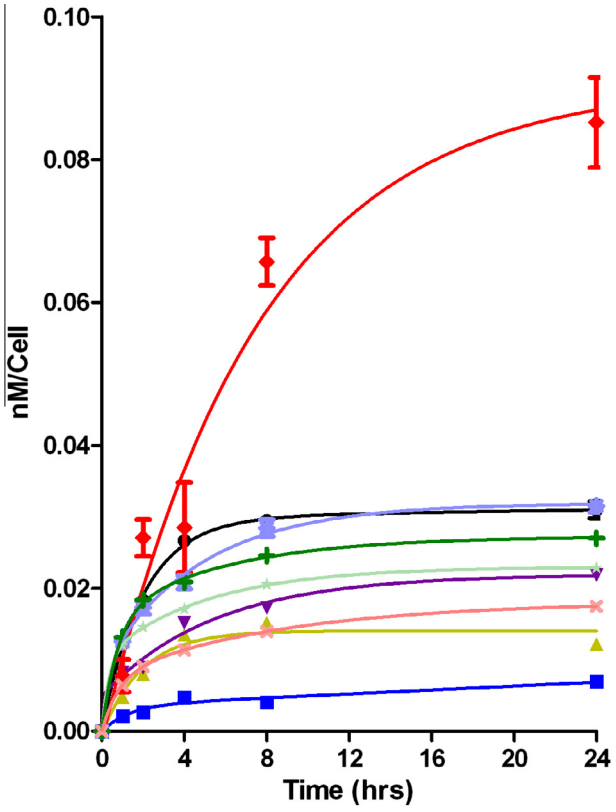

Figure 4. Time-dependent uptake of *meso*-aryl-BODIPYs **1a** (black), **2a** (blue), **4a** (yellow), **5** (light purple), **6a** (purple), **7** (light green), **8** (dark green), **10** (pink) and **10a** (red) at 10 μM by human HEp2 cells.

phototoxic, probably due to its highly lipophilic nature and lack of peripheral functionalization that might favor protein binding.[54] On the other hand, BODIPY **7a** bearing a *meso*-thienyl group was the poorest generator of singlet oxygen ($\Phi_\Delta = 0.02$) but still showed high phototoxicity (and low dark toxicity), indicating different mechanism(s) for cell photosensitization.

4. Conclusions

A series of eleven photo-stable *meso*-aryl-BODIPYs, bearing both *meso*-phenyl and *meso*-thienyl groups, were synthesized and iodinated at the 2,6-positions to investigate the effect of the iodine atoms and the nature of the *meso*-aryl group on their photophysical properties and cytotoxicity. BODIPYs bearing *meso*-thienyl and *meso*-pentafluorophenyl substituents, showed the largest red-shifted absorptions and emissions due to their lower HOMO–LUMO gap, as determined computationally. The 2,6-diiodo-BODIPYs showed lower HOMO and LUMO energies compared with the corresponding non-iodinated derivatives. Furthermore, *meso*-thienyl BODIPYs showed drastically reduced fluorescence quantum yields due to the greater freedom of rotation of the small thienyl group. Addition of bromine onto the *meso*-substitutent had only a slight effect on the rotational barrier and the fluorescence quantum yields.

Studies in human HEp2 cells revealed that all BODIPYs with exception of **10a** were non-toxic in the dark (IC_{50} >400 μM). Upon light treatment (1.5 J/cm^2) the β-free BODIPYs showed low cytotoxicity (IC_{50} >80 μM) and five of the 2,6-diiodo BODIPYs (**3a**, **5a**, **8a**, **9a** and **11a**) showed no phototoxicity up to 200 μM. On the other hand, six of the 2,6-diiodo-BODIPYs (**1a**, **2a**, **4a**, **6a**, **7a** and **10a**) showed IC_{50} = 3.5–28 μM at 1.5 J/cm^2, demonstrating the significant effect of both the 2,6 diiodo and the *meso*-aryl groups on the cytotoxic properties of BODIPYs. BODIPYs **2a** and **4a** had the highest dark/phototoxicity ratio (>50), and are the most promising for PDT. The high dark and phototoxicity observed for BODIPY **10a** are probably due to its very high cellular uptake, and preferential accumulation within the cell mitochondria.

Acknowledgments

This work was supported by the National Science Foundation, Grant number CHE-0611629. The authors thank the Louisiana Optical Network Initiative for the use of the computer facilities.

Supplementary data

Supplementary data (absorption and emission Figures for all β-free BODIPYs and absorption Figures for all di-iodo-BODIPYs in dichloromethane and THF, ^{1}H and ^{13}C NMR, cytotoxicity plots and X-ray crystal structure reports) associated with this article can be found, in the online version, at http://dx.doi.org/10.1016/j.bmc.2013.07.017.

References and notes

1. Loudet, A.; Burgess, K. *Chem. Rev.* **2007**, *107*, 4891.
2. Ulrich, G.; Ziessel, R.; Harriman, A. *Angew. Chem., Int. Ed.* **2008**, *47*, 1184.
3. Benstead, M.; Mehl, G. H.; Boyle, R. W. *Tetrahedron* **2011**, *67*, 3573.
4. Boens, N.; Volker Leen, V.; Dehaen, W. *Chem. Soc. Rev.* **2012**, *41*, 1130.
5. Awuah, S. G.; You, Y. *RSC Adv.* **2012**, *2*, 11169.
6. Kamkaew, A.; Lim, S. H.; Lee, H. B.; Kiew, L. V.; Chung, L. Y.; Burgess, K. *Chem. Soc. Rev.* **2013**, *42*, 77.
7. Dougherty, T. J.; Gomer, C. J.; Henderson, B. W.; Jori, G.; Kessel, D.; Korbelik, M.; Moan, J.; Peng, Q. *J. Nat. Cancer Inst.* **1998**, *90*, 889.
8. Dolmans, D.; Fukumura, D.; Jain, R. K. *Nat. Rev. Cancer* **2003**, *3*, 380.
9. Huang, Z. *Tech. Cancer Res. Treat.* **2005**, *4*, 283.
10. Brown, S. B.; Brown, E. A.; Walker, I. *Lancet Oncol.* **2004**, *5*, 497.
11. Jiao, L.; Li, J.; Zhang, S.; Wei, C.; Hao, E.; Vicente, M. G. H. *New J. Chem.* **2009**, *33*, 1888.
12. Jiao, L.; Yu, C.; Uppal, T.; Liu, M.; Li, Y.; Zhou, Y.; Hao, E.; Hu, X.; Vicente, M. G. H. *Org. Biomol. Chem.* **2010**, *8*, 2517.
13. Ortiz, M. J.; Agarrabeitia, A. R.; Duran-Sampedro, G.; Prieto, J. B.; Lopez, T. A.; Massad, W. A.; Montejano, H. A.; García, N. A.; Arbeloa, I. L. *Tetrahedron* **2012**, *68*, 1153.
14. Yogo, T.; Urano, Y.; Ishitsuka, Y.; Maniwa, F.; Nagano, T. *J. Am. Chem. Soc.* **2005**, *127*, 12162.
15. Lim, S. H.; Thivierge, C.; Nowak-Sliwinska, P.; Han, J.; van den Bergh, H.; Wagnières, G.; Burgess, K.; Lee, H. B. *J. Med. Chem.* **2010**, *53*, 2865.
16. Pandey, S. K.; Pan, S.; Kant, R.; Kuruvilla, S. A.; Pan, M.-L.; Mukherjee, J. *Bioorg. Med. Chem. Lett.* **2012**, *22*, 7610.
17. Darwish, A.; Blacker, M.; Janzen, N.; Rathmann, S. M.; Czorny, S.; Hillier, S. M.; Joyal, J. L.; Babich, J. W.; Valliant, J. F. *ACS Med. Chem. Lett.* **2012**, *3*, 313.
18. Tanaka, M.; Uehara, S.; Kojima, A.; Matsumoto, M. *Phys. Med. Biol.* **2007**, *52*, 4409.
19. Agdeppa, E. D.; Spilker, M. E. *AAPS J.* **2009**, *11*, 286.
20. Lumcke, S.; Hönnscheidt, C.; Waschatko, G.; Bopp, A.; Lütjohann, D.; Bertram, N.; Gehrig-Burger, K. *Mol. Cell Endocrinol.* **2010**, *314*, 31.
21. Lund, F. W.; Lomholt, M. A. *BMC Biophys.* **2012**, *5*, 20.
22. Beatty, K. E.; Szychowski, J.; Fisk, J. D.; Tirrell, D. A. *Chem. BioChem.* **2011**, *12*, 2137.
23. Atilgan, S.; Ekmekci, Z.; Dogan, A. L.; Gucb, D.; Akkaya, E. U. *Chem. Commun.* **2006**, 4398.
24. He, H.; Lo, P.-C.; Yeung, S.-L.; Fong, W.-P.; Ng, D. K. P. *Chem. Commun.* **2011**, 4748.
25. Uppal, T.; Bhupathiraju, N. V. S. D. K.; Vicente, M. G. H. *Tetrahedron* **2013**, *69*, 4687.
26. Yang, F.; Xu, X. L.; Gong, Y. H.; Qiu, W. W.; Sun, Z. R.; Zhou, J. W.; Audebert, P.; Tang, J. *Tetrahedron* **2007**, *63*, 9188.
27. Kollmannsberger, M.; Rurack, K.; Resch-Genger, U.; Daub, J. *J. Phys. Chem. A* **1998**, *102*, 10211.
28. Jiao, L.; Yu, C.; Li, J.; Wang, Z.; Wu, M.; Hao, E. *J. Org. Chem.* **2009**, *74*, 7525.
29. Ozdemir, T.; Atilgan, S.; Kutuk, I.; Yildirim, L. T.; Tulek, A.; Bayindir, M.; Akkaya, E. U. *Org. Lett.* **2009**, *11*, 2105.
30. Wang, J. G.; Hou, Y. J.; Li, C.; Zhang, B. W.; Wang, X. S. *Sens. Actuators, B-Chem.* **2011**, *157*, 586.
31. Qin, W.; Baruah, M.; De Borggraeve, W. M.; Boens, N. *J. Photochem. Photobiol., A: Chem.* **2006**, *183*, 190.
32. Zhang, X. L.; Xiao, Y.; Qian, X. H. *Org. Lett.* **2008**, *10*, 29.

33. Jun, T.; Kim, K.; Lee, K. M.; Benniston, A. C.; Churchill, D. G. *J. Coord. Chem.* **2012**, *65*, 4299.
34. Alamiry, M. A. H.; Benniston, A. C.; Hagon, J.; Winstanley, T. P. L.; Lemmetyinen, H.; Tkachenko, N. V. *RSC Adv.* **2012**, *2*, 4944.
35. Zhang, D.; Wang, Y.; Xiao, Y.; Qian, S.; Qian, X. *Tetrahedron* **2009**, *65*, 8099.
36. Ye, J. H.; Hu, Z. J.; Wang, Y. X.; Zhang, W. C.; Zhang, Y. *Tetrahedron Lett.* **2012**, *53*, 6858.
37. Sabatini, R. P.; McCormick, T. M.; Lazarides, T.; Wilson, K. C.; Eisenberg, R.; McCamant, D. W. *J. Phys. Chem. Lett.* **2011**, *2*, 223.
38. Mathai, S.; Smith, T. A.; Ghiggino, K. P. *Photochem. Photobiol. Sci.* **2007**, *6*, 995.
39. Didier, P.; Ulrich, G.; Mély, Y.; Ziessel, R. *Org. Biomol. Chem.* **2009**, *7*, 3639.
40. Becke, A. D. *J. Chem. Phys.* **1993**, *98*, 5648.
41. Lee, C.; Yang, W.; Parr, R. G. *Phys. Rev. B* **1988**, *37*, 785.
42. Stevens, W. J.; Basch, H.; Krauss, M. *J. Chem. Phys.* **1984**, *81*, 6026.
43. Stevens, W. J.; Krauss, M.; Basch, H.; Jasien, P. G. *Can. J. Chem.* **1992**, *70*, 612.
44. Cundari, T. R.; Stevens, W. J. *J. Chem. Phys.* **1993**, *98*, 5555.
45. Frisch, M. J.; Trucks, G. W.; Schlegel, H. B.; Robb, M. A.; Cheeseman, J. R.; Scalmani, G.; Barone, V.; Mennucci, B.; Petersson, G. A.; Nakatsuji, H.; Caricato, M.; Li, X.; Hratchian, H. P.; Izmaylov, A. F.; Bloino, J.; Zheng, G.; Sonnenberg, J. L.; Hada, M.; Ehara, M.; Toyota, K., Fukuda, R.; Hasegawa, J.; Ishida, M.; Nakajima, T.; Honda, Y.; Kitao, O.; Nakai, H.; Vreven, T.; Montgomery, J. A.; Peralta, J. E.; Ogliaro, F.; Bearpark, M.; Heyd, J. J.; Brothers, E.; Kudin, K. N.; Staroverov, V. N.; Kobayashi, R.; Normand, J.; Raghavachari, K.; Rendell, N.; Burant, J. C.; Iyengar, S. S.; Tomasi, J.; Cossi, M.; Rega, N.; Millam, J. M.; Klene, N.; Knox, J. E.; Cross, J. B.; Bakken, V.; Adamo, C.; Jaramillo, J.; Gomperts, R.; Stratmann, R. E.; Yazyev, O.; Austin, A. J.; Cammi, R.; Pomelli, C.; Ochterski, J. W.; Martin, R. L.; Morokuma, K.; Zakrzewski, V. G.; Voth, G. A.; Salvador, P.; Dannenberg, J. J.; Dapprich, S.; Daniels, A. D.; Farkas, O.; Foresman, J. B.; Ortiz, J. B.; Cioslowski, J.; Fox, D. J. Gaussian, Inc.: Wallingford CT, 2009.
46. Meng, G.; Velayudham, S.; Smith, A.; Luck, R.; Liu, H. Y. *Macromolecules* **2009**, *42*, 1995.
47. Mula, S.; Ray, A. K.; Banerjee, M.; Chaudhuri, T.; Dasgupta, K.; Chattopadhyay, S. *J. Org. Chem.* **2008**, *73*, 2146.
48. Uppal, T.; Hu, X.; Fronczek, F. R.; Maschek, S.; Bobadova-Parvanova, P.; Vicente, M. G. H. *Chem. Eur. J.* **2012**, *18*, 3893.
49. Rihn, S.; Retailleau, P.; Bugsaliewicz, N.; De Nicola, A.; Ziessel, R. *Tetrahedron Lett.* **2009**, *50*, 7008.
50. Fu, L.; Jiang, F.-L.; Fortin, D.; Harvey, P. D.; Liu, Y. *Chem. Commun.* **2011**, 5503.
51. Qu, X. Y.; Liu, Q.; Ji, X. N.; Chen, H. C.; Zhou, Z. K.; Shen, Z. *Chem. Commun.* **2012**, 4600.
52. Benniston, A. C.; Copley, G. *Phys. Chem. Chem. Phys.* **2009**, *11*, 4124.
53. Kim, K.; Jo, C.; Easwaramoorthi, S.; Sung, J.; Kim, D. H.; Churchill, D. G. *Inorg. Chem.* **2010**, *49*, 4881.
54. Yogo, T.; Urano, Y.; Mizushima, A.; Sunahara, H.; Inoue, T.; Hirose, K.; Lino, M.; Kikuchi, K.; Nagano, T. *PNAS* **2008**, *105*, 28.
55. Weissig, V. *Exp. Opin. Drug Delivery* **2005**, *2*, 89.
56. Kessel, D.; Luo, Y. *J. Photochem. Photobiol., B: Biol.* **1998**, *42*, 89.
57. Kochevar, I. E.; Redmond, R. W. *Methods Enzymol.* **2000**, *319*, 20.
58. Huang, L.; Zhao, J.; Guo, S.; Zhang, C.; Ma, J. *J. Org. Chem.* **2013**, *78*, 5627.